Journal of Hydrology: Regional Studies 50 (2023) 101524

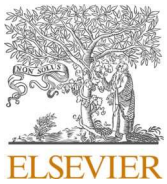

Contents lists available at ScienceDirect

Journal of Hydrology: Regional Studies

journal homepage: www.elsevier.com/locate/ejrh

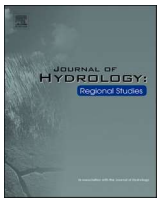

Evaluation of meteorological microphysical schemas based on the WRF model for simulation of rainfall in the northeastern region of Iran

Rasoul Sarvestan [a], Mokhtar Karami [a,*,1], Reza Javidi Sabbaghian [b]

[a] Department of Climatology, Faculty of Geography & Environmental Sciences, Hakim Sabzevari University, Sabzevar, Iran
[b] Department of Civil Engineering, Hakim Sabzevari University, Sabzevar, Khorasan Razavi, Iran

ARTICLE INFO

Keywords:
Weather Research and Forecasting model
Climatic types
Rainfall simulation
Flood control
Khorasan Razavi Province

ABSTRACT

Study region: The Khorasan Razavi Province represents a variety of climatic types in the northeastern region of Iran. It lies between 56° 19′ and 61° 16′ east longitude and 33° 52′–37° 42′ north latitude, which is one of the largest and most densely populated provinces in Iran.
Study focus: The aim of this study is using the Weather Research and Forecasting (WRF) model to evaluate and simulate rainfall in the northeastern region of Iran based on the climatic conditions in order to rainfall forecasting, also warn about and control probable floods.
New hydrological insights for the region: Following the climatic classification of the study area, the six WRF model schemas were employed to implement the model in this area: Purdue-Lin (Lin), WRF Single-Moment class 3, 5, 6 (WSM3, WSM5, WSM6), and WRF Double-Moment class 5, 6 (WDM5, WDM6). The results revealed that the Threat Score (TS) coefficients for the WDM5 and Lin schemas in the desert climate are 1 and 0.97, respectively; the TS coefficient for each one of the Lin, WSM3, and WDM6 have the value of 0.60 in the semi-desert climate. The Lin scheme performs the best in all climates of the study area. The results revealed that the WRF model accurately simulates rainfall in the climatic conditions of the region. Hydrologists and planners will be able to use this meteorological model as an input to hydrological models based on the output of the WRF model, which can provide early flood warnings within the next 24 h based on these findings.

1. Introduction

Flooding is one of the most devastating natural disasters in the world that causes casualties, economic losses and societal impacts on the human life. In recent years, the flood events in several regions of the world especially in urban watersheds have become more intense and frequent as the result of climate change and human intervention such as the related land use changes. Furthermore, even formerly less vulnerable regions may be subjected to future intensive rainfall and the relevant floods (Fatti et al., 2013). According to the many studies, rainfall is counted as the most effective component of the hydrological processes, also the most important source of flood events causing large-scale flooding and landslides in regions around the world, every year (Evans et al., 2000; Cong et al., 2006;

* Corresponding author.
E-mail addresses: M.Karami@hsu.ac.ir, M.Karami08@Yahoo.co.uk (M. Karami).
[1] ORCID iD: 0000-0001-8336-3621.

https://doi.org/10.1016/j.ejrh.2023.101524
Received 13 January 2023; Received in revised form 15 July 2023; Accepted 2 September 2023

Casagli et al., 2006; Chen and Hossain, 2018). The human and financial repercussions caused by floods can be minimized based on accurate simulating rainfall and its reliable forecasting, as an effective and efficient strategy for flood risk mitigation (Khan et al., 2014; Jha and Afreen, 2020). Accordingly, as the most important step of the meteorological analysis process, an accurate and reliable model should be developed to simulate and forecast rainfall and estimate its spatial and temporal distribution in order to compute generated runoff in hydrological applications (Givati et al., 2011). In addition, the rainfall forecasting models are so important for flash flooding areas where the hydrological responses are rapid and extreme (Douinot et al., 2016; Tian et al., 2019). Therefore, applying Numerical Weather Prediction (NWP) is useful for flood forecasting in several regions of the world (Cluckie and Han, 2000; Liu et al., 2013).

Numerical forecasting models can improve the accuracy and reliability of flood forecasts by connecting meteorological to hydrological data (Wu et al., 2014; Yesubabu et al., 2016). Moreover, the recent modern computing power beside the ability of mesoscale numerical weather models enable higher resolution rainfall simulations and forecasts in space and time (Liu et al., 2012). Recently, forecasting reliability has also increased due to advances in meteorological and hydrological models, satellite data collection, and uncertainty analysis methods (Jain et al., 2018).

Related to using numerical weather and forecasting models, it is significant the consideration of the variations in rainfall and runoff trends in several areas depending on the climatic conditions (Masaki et al., 2014; Andimuthu et al., 2019). These changes would affect climate-sensitive areas such as arid and semi-arid regions, which increases surface erosion and flooding in types of climates (Peterson and Wicks, 2006; Zahmatkesh et al., 2015; Andimuthu et al., 2019). Regarding this, Alfieri et al. (2013) presented the Global Flood Awareness System (GloFAS) to provide an overview of future floods in broad globe river basins. The GloFAS is based on a distributed hydrological simulation of global numerical weather predictions. Accordingly, their findings suggested the Weather Research and Forecasting (WRF) model that estimates rainfall in better accurate with more reliability in comparison with the satellite image processing. Also, the findings revealed that the WRF model could be employed independently in a variety of marine and tropical climates.

A comprehensive review of the recent studies also demonstrates that the most of them have used various meteorological models to manage floods in several regions of the world. As the result, the WRF model, which has numerous schemas based on the climatic conditions of different world locations, is one of the most important and practical meteorological models. The most important recent studies on a worldwide scale about the rainfall simulation and forecasting are summarized in Table 1.

Regarding with the previous studies, it is received that the most of them have applied the statistical models for rainfall simulation and its forecasting with higher approximations and more uncertainties. Also, the previous numerical studies have mostly focused on selection of the schemas in the urban regional scale, not in the climatic scale. This study uses the WRF dynamic microscale numerical model to achieve higher accuracy and reliability by selection of the most desirable scheme for each climatic type based on the verification process. Accordingly, the probable rainfalls could be forecasted once each scheme is determined in various climatic conditions. The forecasted rainfall outputs from the numerical meteorological WRF model can be connected as the inputs to the hydrological models to estimate future runoff to better manage probable floods and mitigate the related risks.

Regarding this research importance, the northeastern region of Iran, as its geographical location, differences in topography and the variety of climatic conditions, faces the risk associated with the flood events that recently caused to relevant human casualties and heavy financial damages. On the other hand, the weather is generally forecasted for the whole Khorasan Razavi Province, therefore it is not forecasted for the cities and the climatic types, independently. Consequently, due to the area size and the variety of several climatic

Table 1
The most important recent studies on rainfall simulation and forecasting in several regions of the world.

Case study	Model	Description	Authors
Gopalpur	WRF	The results demonstrated that the WSM3 micro-physical schema accurately simulates tropical storm tracks and intensity.	Mahala et al. (2015)
North West Iran	WRF	The results demonstrated that cumulus schemas are more sensitive, while microphysical schemas are less sensitive.	Zeyaeyan et al. (2017)
South Western of Iran	WRF, ANN[a], SVM[b]	This study employed the three short-term meteorological forecasting models to predict floods. The results demonstrated that the WRF model schema has higher accuracy than the SVM and ANN models.	Shirali et al. (2020a)
Northern Iran	WRF	According to the results of this work and the ability of the used forecasting model, the Grell-Devenyi schema has the superior configuration in the rainfall simulation seen from the event in the region.	Khansalari et al. (2021)
North-Western Himalaya	WRF	This study demonstrated how an integrated method could be employed to provide rapid flood warnings in mountainous areas.	Thakur et al. (2018)
Sinai Peninsula	WRF	This study developed a model to predict heavy rainfall in the same way that Sinai did. The relevant results revealed that the WRF model had a high level of accuracy in forecasting short-term precipitation and associated rain, which resulted in flooding in this area.	El Afandi and Morsy (2020)
Northern Tunisia.	WRF, ECMWF[c]	The results demonstrated that WRF model schemas could estimate rainfall in northern Tunisia.	Dhib et al. (2021)
Eastern Nile, Egypt	WRF, SWAT	The results indicated that the bias-corrected precipitation Felds from WRF can contribute to improved hydrological impact assessments.	Osman et al. (2021)
Cyprus	WRF	The results select an efficient set of WRF Multiphysics configurations that accounts for these properties and that can be used as input for hydrologic.	Sofokleous et al. (2021)

[a] Artificial Neural Network.
[b] Support Vector Machine.
[c] European Centre for Medium-Range Weather Forecasts.

conditions, the forecasting reports usually have little reliability for the cities in the study area. Accordingly, one of the approaches for accurate forecasting, reduction of flood losses and damages, and effective flood management at the local scale, is the determination of desirable schemas for climatic conditions at the local level. To achieve this goal, first, by classifying and identifying the different climates of the region on the local scale, the dynamic meteorological modeling based on micro-scale is implemented. Then, according to the verification criteria for the model, the optimal scheme corresponding to each of the climatic conditions in the study area is selected. Finally, the relevant scheme can be used for reliable short-term weather forecast at the local scale and urban level to effective flood management in future.

The paper is organized as follows. Section 2, introduces the study area and presents the used data, also, describes the WRF model, the verification methods, and the climate classification. Section 3, presents the results of the WRF simulations, comparing the six microphysical schemas with the six verification methods, and discusses about the results. A summary of the conclusions and the suggestions for future studies are included in Section 4.

2. Research methods

2.1. Study area

Khorasan Razavi Province is located in northeastern Iran, and it is one of the country's largest and most densely populated regions, with latitude ranging from 56° 19′ to 61° 16′ east and longitude ranging from 33° 52′ to 37° 42′ north. This province's centre is Mashhad. This province is the fourth largest in the country, with an area of 118,854 square kilometers. On the north and northeast, the province shares a 6531-kilometer border with Turkmenistan, while on the east, it shares a 302-kilometer border with Afghanistan. The study area has been restricted to Turkmenistan to the north, Afghanistan to the east, Semnan to the west, and Southern Khorasan and Yazd to the south and southwest, respectively (Statistical yearbook, 2019). The climate of Khorasan Razavi Province is diverse, as seen below (Meteorological, 2020). (Fig. 1). The province's size and characteristics, such as high mountains and desert parts, distance from the sea, and varying winds, have resulted in diverse climates in its regions. This province receives a moderate amount of rainfall and humidity. Quchan City receives the highest annual rainfall (296 mm), while Gonabad City receives the least annual rainfall (71 mm) among the centers of cities with meteorological stations (https://fa.wikipedia.org/wiki/2019). The population of Razavi Khorasan is equal to 6,434,501 people according to the latest population and housing census (2016), which is the second province of Iran in terms

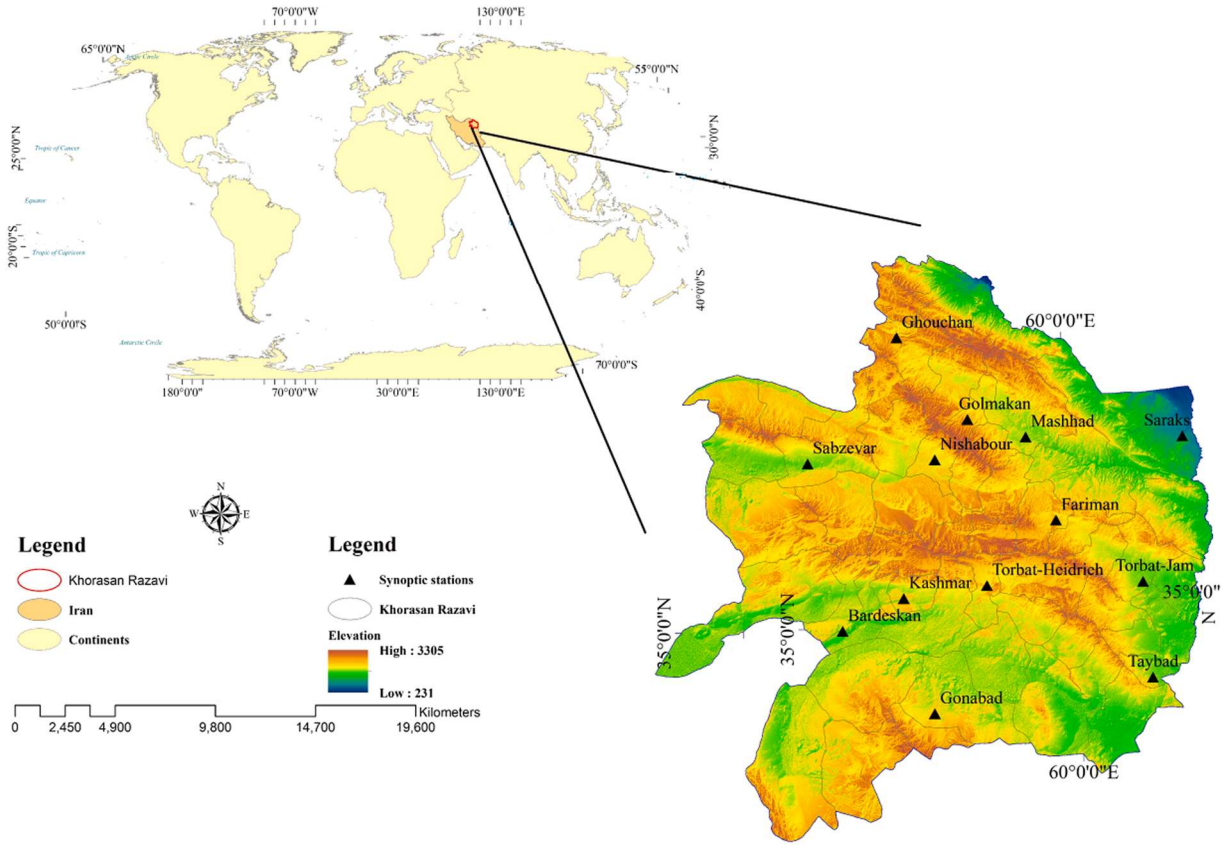

Fig. 1. The location of Khorasan Razavi Province in northeastern Iran and in the global map.

of population. The city of Mashhad, which is the centre of of Khorasan Razavi, is also considered the largest city of this province, with a population of 3,001,184 people (equivalent to 46.1 % of the province's population) (Housing Population Statistics, 2016).

2.2. Datasets

Precipitation analysis requires two types of data: observational data and Hamadi forecast system data.

2.2.1. Observational data

Table 2, presents the five most severe events that occurred in the Khorasan Razavi Province in the winter, spring, and summer of 2019 and 2020, which are related to the 13 synoptic stations and the relevant properties. According to the spatial data collected from the 13 synoptic stations from 2019 to 2020, which are used for the rainfall simulation process, Figs. 2(a) and 2(b) have been provided to represent the distribution of annual rainfall and the classification of climatic conditions of the study area, respectively.

It is noted that the available observational data related to the events received from the 13 synoptic stations of the study area are the cumulative 24-h rainfall. It is due to that the cumulative precipitation helps to choose the more accurate scheme for climates, as presented by the recent studies that have used the WRF meteorological model (Agogbuo et al., 2017; Karki et al., 2018; Mekawy et al., 2022; Sarvestan et al., 2023). Also, regarding that, the goal of this research is not to analyze the frequency and intensity of rainfall, there is no significant difference in rainfall intensity under different climatic conditions during the rainfall duration, and the main objective is just to estimate the accurate and desirable scheme for a large climatic region, the rainfall duration is not important in selecting the scheme type (Faiers et al., 1994; Mishra et al., 2012; Clark and Dent, 2021). Furthermore, this research aims to identify the most desirable scheme according to the type of climate to predict precipitation in the next 24 h, considering the computational operations in different stages and its results in a large area (at the provincial level), so the rainfall duration is not specified.

2.2.2. Hamadi forecast system data

The six distinct schemas are investigated for the model in this study. In addition, the following two domains are employed in this study:

a) A 15 km by 15 km region with a latitude of 24–42° north and a longitude of 42–66° east within Iran (Fig. 3a).

b) A 5 km by 5 km region with a latitude of 31–42° north and a longitude of 53–63° east in Khorasan Razavi (Fig. 3b).

Regarding Fig. 3, it is noted that the WRF model as a dynamic downscaling model requires a wider domain than the study area to simulate and predict precipitation, accurately. Also, the domain is square and cannot be chosen in a polygonal way, so it has to cover the entire study area and some surrounding areas. Furthermore, the climate of the study area does not include any water body area or marine climatic conditions, so the presence of the Caspian Sea in the domain does not affect the results.

2.3. The WRF model

The Weather Research and Forecasting (WRF) model, as the next-generation mesoscale numerical weather prediction (NWP) system, is applied for meteorological research and operational forecasting. This model is also counted as one of the dynamic downscaling models. Since the dynamic downscaling WRF model converts larger grids into smaller grids at the regional and local scale in meteorological simulation and forecasting, this model can be used for transboundary regions such as the study area. It has two dynamical cores, including a data assimilation system and architecture software that facilitates parallel computation and system

Table 2
The properties of the synoptic stations and the observational precipitation related to the five events in the study area.

Station No.	Station name	Longitude	Latitude	Altitude (m)	Selected events (mm)				
					31 Oct 2019	12 Jan 2020	26 Feb 2020	24 May 2020	12 April 2020
1	Torbat_Jam	60°35′	35°15′	950	24	3	2	13.3	2.2
2	Torbat_Haydariyeh	59°13′	35°16′	1451	24	4	0.3	29.2	2.3
3	Sabzevar	57°43′	36°12′	972	10	15	4	36	28.2
4	Sarakhs	61°10′	31°12′	280	24	9	0.1	27.2	0.8
5	Quchan	58°30′	37°40′	1287	18.5	0	13	9	23
6	Kashmar	58°28′	35°12′	1110	27.2	6	0.6	34.2	6.6
7	Golmakan	59°17′	36°29′	1176	14.5	2	41	17.9	14
8	Gonabad	58°41′	34°21′	1056	24.1	0.1	9	23.3	0.3
9	Mashhad	36°16′	59°38′	999	12.5	0	8	29.8	3.5
10	Neyshabour	58°48′	36°16′	1213	0	0	3	22.2	17.2
11	Fariman	59°50′	35°30′	1400	16.2	0.1	6	17.3	6.9
12	Taybad	60°47′	34°44′	900	18.2	0	19	37.9	1.1
13	Bardeskan	57°57′	35°16′	1011	31	0.8	12	29.3	0.7

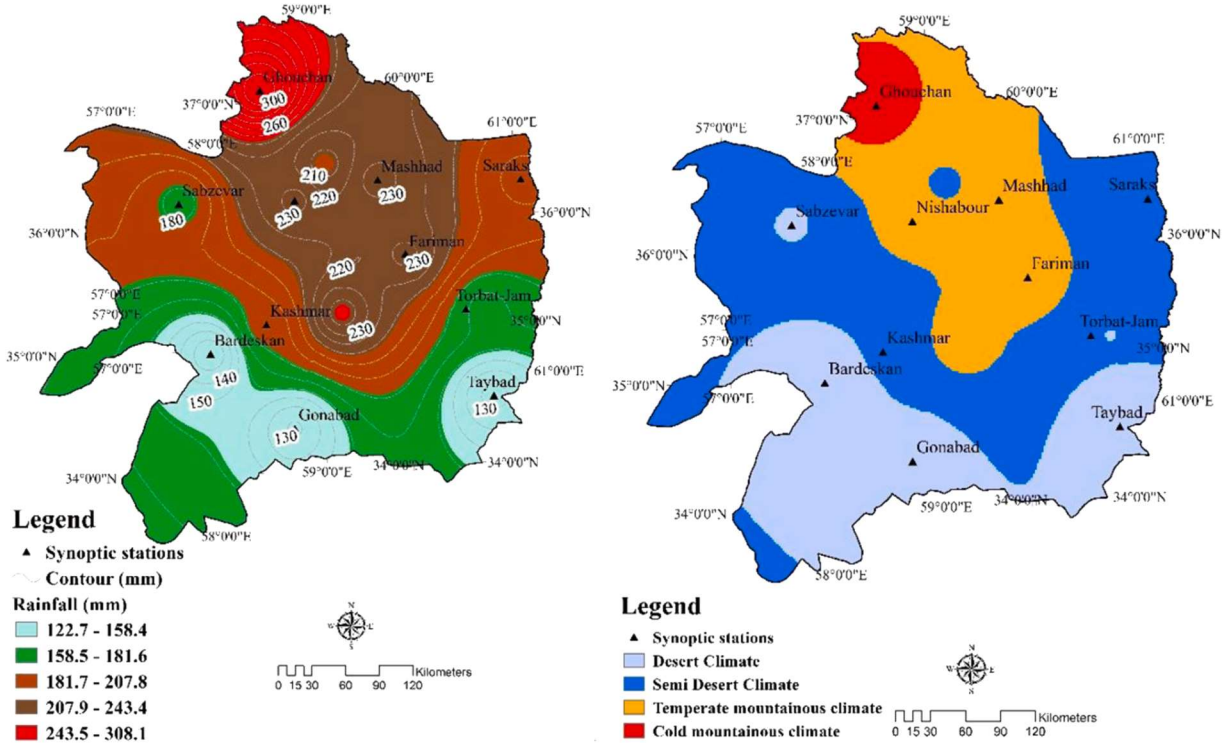

Fig. 2. **(a)** The distribution of annual rainfall and **(b)** The classification of climatic conditions in the study area.

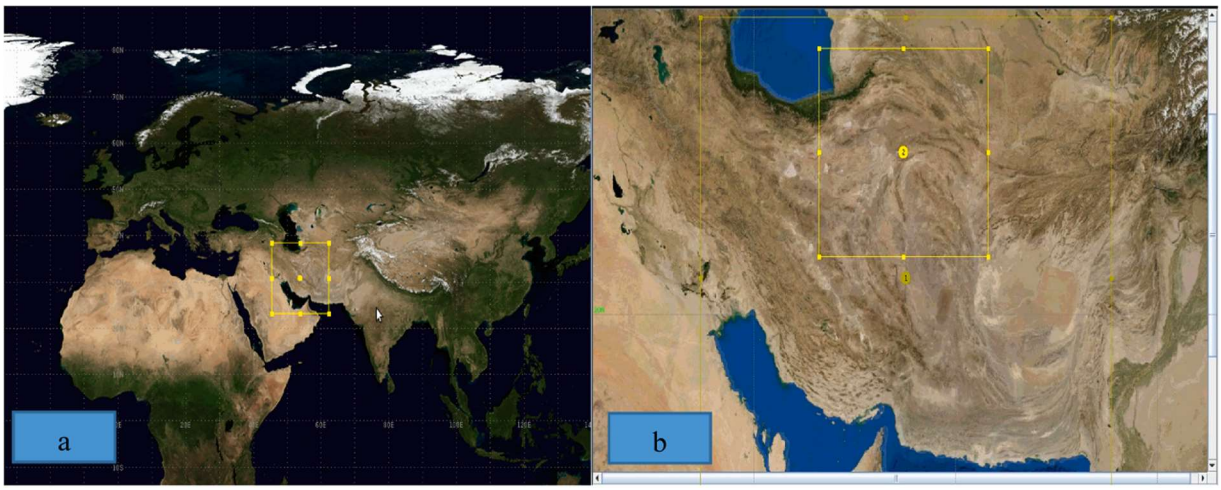

Fig. 3. **(a)** The outer domain of the WRF model and **(b)** the inner domain of the WRF model.

extensibility. The model can also be used for a wide range of meteorological applications, from tens of meters to thousands of kilometers(www.mmm.ucar.edu/weather-research-and-forecasting-model). The WRF version 4.5.1 is used to simulate actual atmospheric conditions or idealized feasible conditions during the model process (Zhang et al., 2021; Langkamp and Böhner, 2011). Also, in association with the type of variables in the WRF model, the prognostic variables consist of velocity components of u and v in Cartesian coordinates, vertical velocity of w, perturbation potential temperature, perturbation geopotential and perturbation surface pressure of arid air, as well as several optional prognostic variables depending on the physical model options (Zhang et al., 2021; Skamarock et al., 2005, 2008; Wong et al., 2012).

This paper compares the rainfall simulations with the observational data from the 13 synoptic stations of the study area using the six schemas: WSM3, WSM5, WSM6 (Hong and Lim, 2006; Hong et al., 2004; Naing, 2021), WDM5 (Wang et al., 2011; Mahala et al., 2021), WDM6 (Guo et al., 2019; Hong et al., 2010), and Lin (Cao et al., 2021). Each of these schemas analyzes the microphysical

schemes of the study area. Then, for each of the climate types, it is determined which schematic representation forecasts rainfall with desirable reliability. Table 3 summarizes the configuration and execution elements of the WRF model.

2.4. The verification of simulation

The Simulation verification is a step to evaluate the model performance and reliability of simulated meteorological output by comparing it with observational data. This ensures that the future projected data can become accurate and reliable. Accordingly, this study uses two approaches for simulation verification including the positive and negative approaches, as described by Mohammadiha et al. (2012), Kodamana and Fletcher (2021), Satya et al. (2021). The positive simulation verification criteria are the Threat Score (TS), Proportion Correct (PC) and Hit rate (Hit). Also, the negative verification criteria are False Alarm Ratio (FAR), False alarm rate (F) and Bias (B). The aforementioned verification criteria are introduced as follows:

2.4.1. Threat Score (TS) coefficient

The Threat Score (TS) coefficient is used to measure the accuracy of predicting a phenomenon occurrence. It is calculated based on dividing the number of days on which the phenomenon is correctly predicted by the total number of days on which the phenomenon occurs or is predicted. Its value varies in the interval of [0,1], where zero means no correct predictions as the worst case and one means all correct predictions as the best case. The TS value is not applicable (NA) when the phenomenon does not occur also is not predicted (Xiefei and Chen, 2020).

2.4.2. Bias (B) coefficient

The Bias (B) coefficient is used to determine how much the average forecasts differ from the average observations. If the Bias is greater (or less) than one, it means that the model overestimates (or underestimates) the number of rainy days at a given threshold compared to the actual number of rainy days at that threshold (Gbode et al., 2019).

2.4.3. False Alarm Ratio (FAR) coefficient

The False Alarm Ratio (FAR) coefficient is the verification metric that is calculated by dividing the number of incorrect predictions by the total number of occurrences. Accordingly, the lower the value, the more favorable the results. It means that the number of zero indicates the best case, while the value of one indicates the worst case (Kodamana and Fletcher, 2021).

2.4.4. Hit rate (H) coefficient

The Hit (H) coefficient is measured by dividing the number of correct predictions of a phenomenon occurrence by the number of phenomenon observations (Letson et al., 2020). This model is also known as the possibility of detection (POD).

2.4.5. False alarm rate (F) coefficient

This verification metric is defined based on the ratio of the total number of incorrect or unfulfilled predictions to the total number of observations that the phenomenon has not occurred (Mohammadiha et al., 2012).

2.4.6. Proportion Correct (PC) coefficient

The Proportion Correct (PC) coefficient is the ratio of correct predictions to the total number of forecasts ( ) (Hadilooie et al., 2014).

The aforementioned verification criteria are presented in Table 4, in which the related matrix variables are defined as follows:

2.5. The De Martonne aridity index

An aridity index is a numerical representation of the degree of aridity in a given environment, which defines the climate type in terms of water availability. The greater the water resource variability, the higher the aridity index of a region (Tabari et al., 2014;

Table 3
Characteristics of the configuration and execution elements of the WRF 5.4.1 model.

Configuration	Outer domain	Inner domain
WRF version	WRF 5.4.1	
Grid spacing (km)	15 km	5 km
Horizontal grids	100 × 132	88 × 100
Vertical grids	42 layer/Top 50 hPa	
Integration time (s)	90	60
spin-up period	24 h	
Radiation	Dudhia short-wave	
Surface layer	5-layer slab, Single-layer, UCM, Monin-Obukhov	
Cumulus	Kain-Fritsch	
Planetary Boundary Layer	Specific Humidity	
Schemas	Lin, WSM3, WSM5, WSM6, WDM5, WDM6	
Initial and boundary conditions	Global Forecasting System (GFS) Model Forecast Fields (27 km resolution, NCEP)	

Table 4
The statistical coefficients applied in the verification method of fence quantities (Mohammadiha et al., 2012).

Verification criteria	Formula	Range	Perfect value
Threat Score (TS)	$TS = \frac{a}{a+b+c}$	0–1	1
Bias (B)	$B = \frac{a+b}{a+c}$	1–∞	1
False Alarm Ratio (FAR)		0–1	0
Hit rate (H)	$H = POD = \frac{a}{a+c}$	0–∞	1
False alarm rate (F)	$F = \frac{b}{b+d}$	0–∞	0
Proportion Correct (PC)	$PC = \frac{a+d}{n}$	0–∞	1

a: The number of times that the phenomenon has occurred and its occurrence has been predicted; b: The number of times that the phenomenon has not occurred, but its occurrence has been predicted; c: The number of times that the phenomenon has occurred but its occurrence has not been predicted; d: The number of times that the phenomenon has not occurred and its occurrence has not been predicted. n: The total number of forecasts (Appendix A. Table 1).

Pellicone et al., 2019). In this study, the climate of the province is classified using the De Martonne classification, with the drought index as the criterion, which is calculated using Eq. (1):

$$Ai = \frac{P}{T+10} \tag{1}$$

where P is the average annual precipitation (mm), and T is the average annual temperature ($^{\circ}C$).

De Martonne establishes thresholds in Eq. (1), resulting in the identification of seven climatic groups ranging from arid to very humid (Appendix A. Table 2). The Emberger thermal divisions are coupled with the original De Martonne climatic classification, resulting in four sub-climates for each climate type: warm, temperate, cold, and ultra-cold.

Therefore, a combination of the two indexes of A_i and t is used to express the reformed De Martonne classification. The first index (A_i) is calculated using aridity index values and the relevant thresholds (Appendix A. Table 2). The second index (M_j) is a thermal index that identifies the sub-climate group to which it belongs (Appendix A. Table 3). The Emberger index, has more or less relevant thresholds, where m is the average daily minimum temperature in the coldest month of the year (Khalili et al., 1991; Zanjani Jam and Sufi, 2016). Finally, both methods are combined as shown in Appendix A. Table 4. To determine the relationship between the De Martonne climatic classification and the Emberger sub-climatic divisions, the climatic zones of the study area are defined. The number of meteorological stations and the statistical period have an impact on the classification of climate zones. This means that they may vary slightly depending on the number of stations or the statistical years used to determine the climate of the region. Therefore, the De Martonne classification method is used in conjunction with the climate of the province.

3. Results and discussion

In general, the climate of the Khorasan Razavi Province is considered semi-arid in Iran. It does, however, have a wide range of climatic conditions. The remaining cities, except Quchan, which has a cold mountainous climate, and Mashhad, Neyshabour, and Fariman, which have a temperate mountainous climate, are in desert or semi-desert climatic conditions, according to the combined De Martonne-Emberger method for climatic classification.

As a result, the climate in most of Khorasan Razavi Province is arid and semi-arid, with drought coefficient values that fall into climatic groups 1 and 2 (Table 5). The eastern and southern parts of the study area are characterized as arid, cold, or desert, according

Table 5
The climatic classification of Khorasan Razavi based on the De Martonne-Emberger method during the 1971–2020.

Climatic category	Station name	T (°C)	P (mm)	M	Climate type
1	Torbat_Haydariyeh	14.2	245.8	-3.9	Desert
	Sabzevar	18.2	176.8	-0.2	
	Gonabad	17.4	128.9	-0.8	
	Taybad	17.9	127	-1.2	
	Bardeskan	19.8	122.7	1.6	
2	Sarakhs	18.2	187.3	1.2	Semi-desert
	Kashmar	17.9	185.8	0.3	
	Torbat_Jam	15.7	166.3	-2.1	
	Golmakan	13.6	205.3	-2.9	
3	Mashhad	15.5	233.8	-1.7	Temperate mountainous
	Neyshabour	14.4	232.6	-3.5	
	Fariman	12.3	232.4	-4.4	
4	Quchan	12.7	308.2	-4.6	Cold mountainous

to the climate analysis.

The northern and central zones are classified as semi-arid, temperate, or desert. Khorasan Razavi is divided into four climate categories: desert, semi-desert, temperate cold, and mountainous cold, according to the findings.

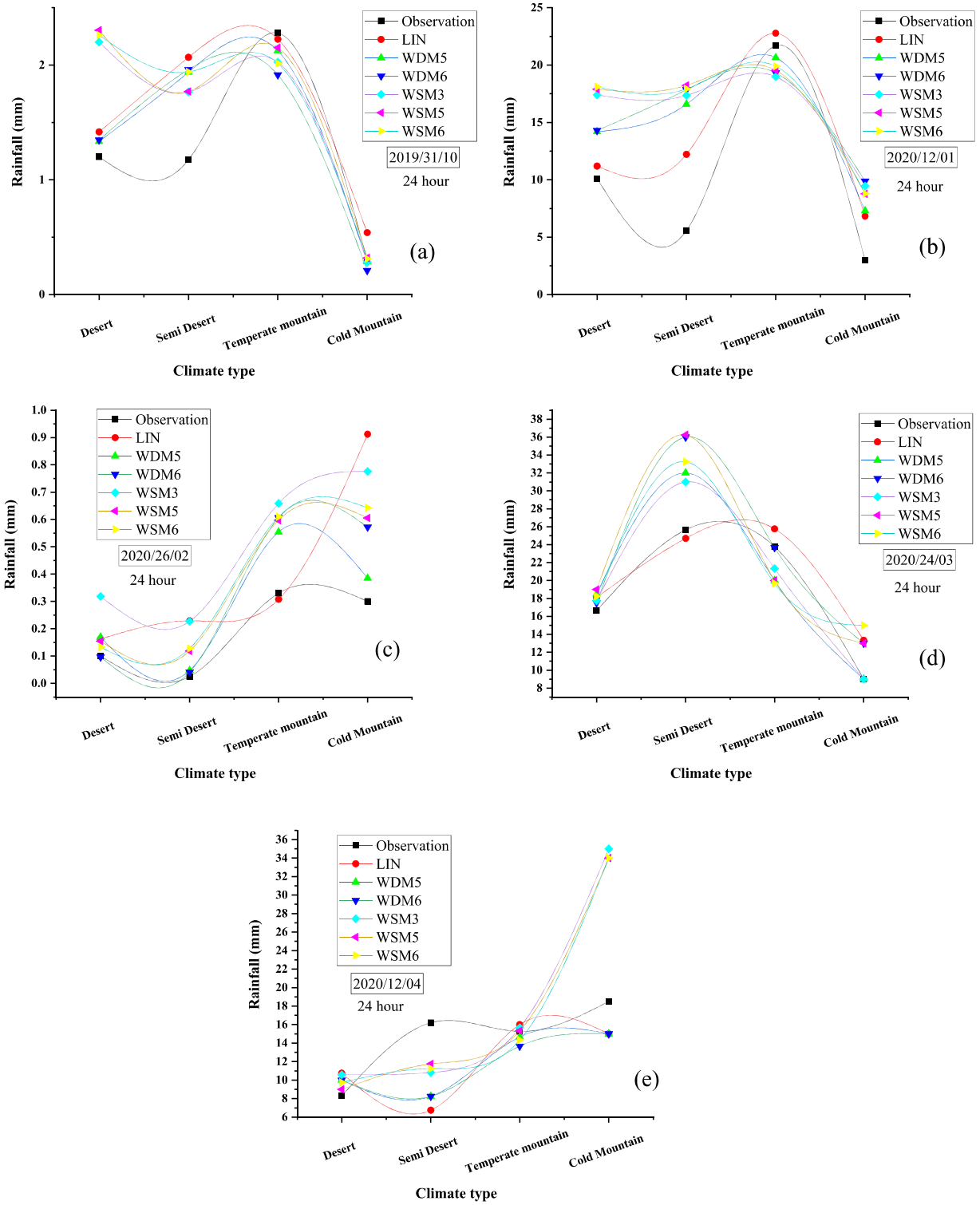

Fig. 4. The WRF model schemas results for the five selected events in each climatic type of the study area.

3.1. Climatic type evaluation

The rainfall values are calculated using the WRF model analysis based on the six schemas once the climate types for the study area have been determined. The comparison between the observational data for five selected events and the model schemas results for each of the climate types of the study area is represented in Fig. 3.

3.1.1. The event 10/31/2019

For the desert climate type, the rainfall simulated using the Lin and WDM5 schemas has the smallest difference with observational data, as shown in Fig. 4a. For the semi-desert climate type, however, the WSM3 and WSM5 schemas exhibit the smallest divergence. Furthermore, for the temperate mountainous climate type, the Lin scheme has the smallest difference with observational data. For the cold mountainous type, however, the simulation results of most of the schemas are quite close to the 24-h observational rainfall. It is worth noting that the semi-desert climate type exhibits the most difference between simulated rainfall and the 24-h observational rainfall among the four climatic conditions. The cold mountainous type, on the other hand, exhibits the most significant concordance between model and data.

3.1.2. The event 01/12/2020

For the desert and semi-desert climate types, the Lin scheme has the smallest difference with 24-h observational rainfall (see Fig. 3). For the temperate mountainous and cold mountainous climate types, the Lin and WDM5 schemas also have the smallest differences with observational data. Furthermore, among the climate types, the semi-desert climate type has the biggest difference between the model results and the observational data, while the temperate mountainous type has the lowest difference.

3.1.3. The event 02/26/2020

The WDM6 scheme has the smallest difference between the simulated rainfall and the cumulative 24-h observational data for the desert climatic condition according to the model results in Fig. 3c, while the WDM5 and WDM6 schemas have the smallest difference for the semi-desert climate type. For temperate mountainous climate type, the Lin scheme has the smallest difference between model results and observational data, whereas the WDM5 scheme has the smallest difference for the cold mountainous climate type. Furthermore, the results show that the cold mountainous type has the highest discordance with observational data, whereas the desert climate type has the lowest.

3.1.4. The event 03/24/2020

Most of the simulation results of the schemas are quite close to the 24-h observational rainfall for the desert climate according to the rainfall simulation results in Fig. 4d, with the Lin scheme having the smallest divergence for the semi-desert climate type. In addition, for temperate mountainous climate type, the WDM6 scheme has the smallest difference with observational data, whereas for cold mountainous climate type, the WSM3 and WDM5 schemas have the smallest difference. The results also show that the semi-desert climate type has the highest difference between model results and observational data among the climate types. The desert and cold mountainous climate types have the smallest.

3.1.5. The event 04/12/2020

The simulation results of most of the schemas, especially for the WSM5 scheme, are quite close to the observational data for the desert and temperate mountainous climate types, according to the model results in Fig. 4e. In the semi-desert climate type, the WSM3, WSM5, and WSM6 schemas have the smallest difference with observational data. For the cold mountainous climate type, the Lin, WDM5, and WDM6 schemas have the smallest differences with observational data. The model results also show that the semi-desert and cold mountainous climate types have the largest difference between model results and observational data, while the desert and temperate mountainous climate types have the smallest.

3.2. Verification criteria

Rainfall forecasting and identification of temporal and spatial patterns have been crucial for flood planning and control, and several researchers have used a variety of approaches to accomplish so (Shirali et al., 2020a, 2020b). However, in this research, the climate types of the regions of the study area are first determined using a combination of the De Martonne-Emberger classification methods. The climatic categorization should then be used to forecast 24-h rainfall. To do this, the rainfall simulation process is used, which is based on the WRF meteorological model schemas on the climate types of the study area. The verification criteria should be used to check the accuracy of using the schemas for rainfall forecasts. In this research, six verification criteria (PC, TS, B, FAR, H, and F) have been used for the accuracy of 24-h rainfall forecasting at the level of the province's climates. The closer the negative values are to zero, it actually indicates the better performance of the meteorological model in predicting rainfall. This mode has the opposite mode for positive quantities. And the closer they are to one, the better the accuracy of the predictions.

Among the negative coefficients, indicate that all of the schemas, especially the Lin and WDM5 schemas, could be almost desirable for simulation in desert regions, according to the verification results presented in Fig. 5 and Table 6. Furthermore, the PC and TS values for the positive coefficients suggest that all of the schemas, particularly the Lin and WDM5, are almost desirable for simulating precipitation in desert climatic conditions.

According to the results of Fig. 5, among the negative coefficients, the B and FAR coefficient values reveal that all of the schemas are

highly desirable for simulating precipitation in temperate mountainous climatic regions. Additionally, the PC coefficient values demonstrate that all of the schemas are appropriate for simulating precipitation, with the WSM6, WDM6, and WDM5 schemas being particularly preferred. All of the schemas are highly desirable based on the TS and H coefficients. Finally, based on the results in of Fig. 5, the B coefficient values indicate that the WDM5, WDM6, and WSM3 schemas are acceptable for simulating, and the Lin scheme

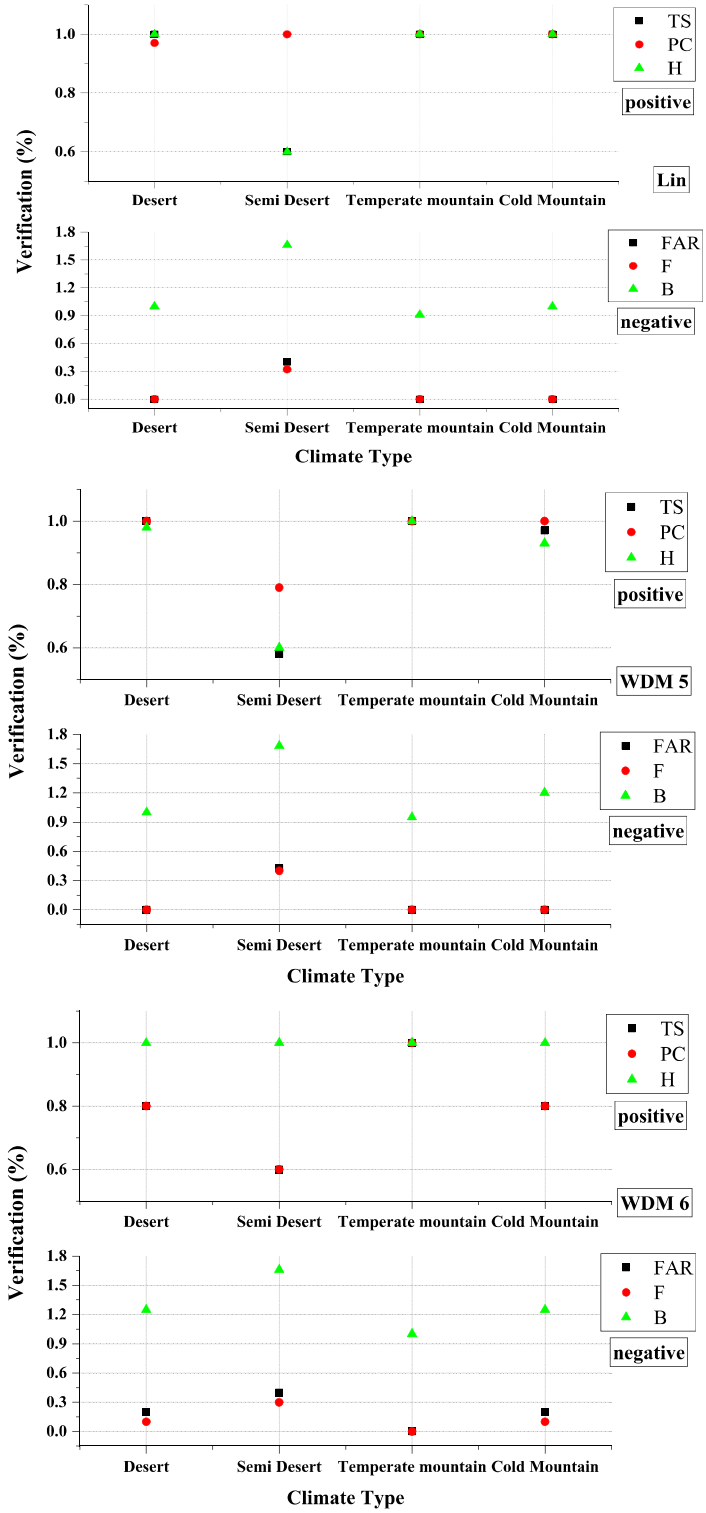

Fig. 5. The verification criteria for the schemas Lin, WDM5, WDM6, WSM3, WSM5 and WSM6 in the four climatic types,.

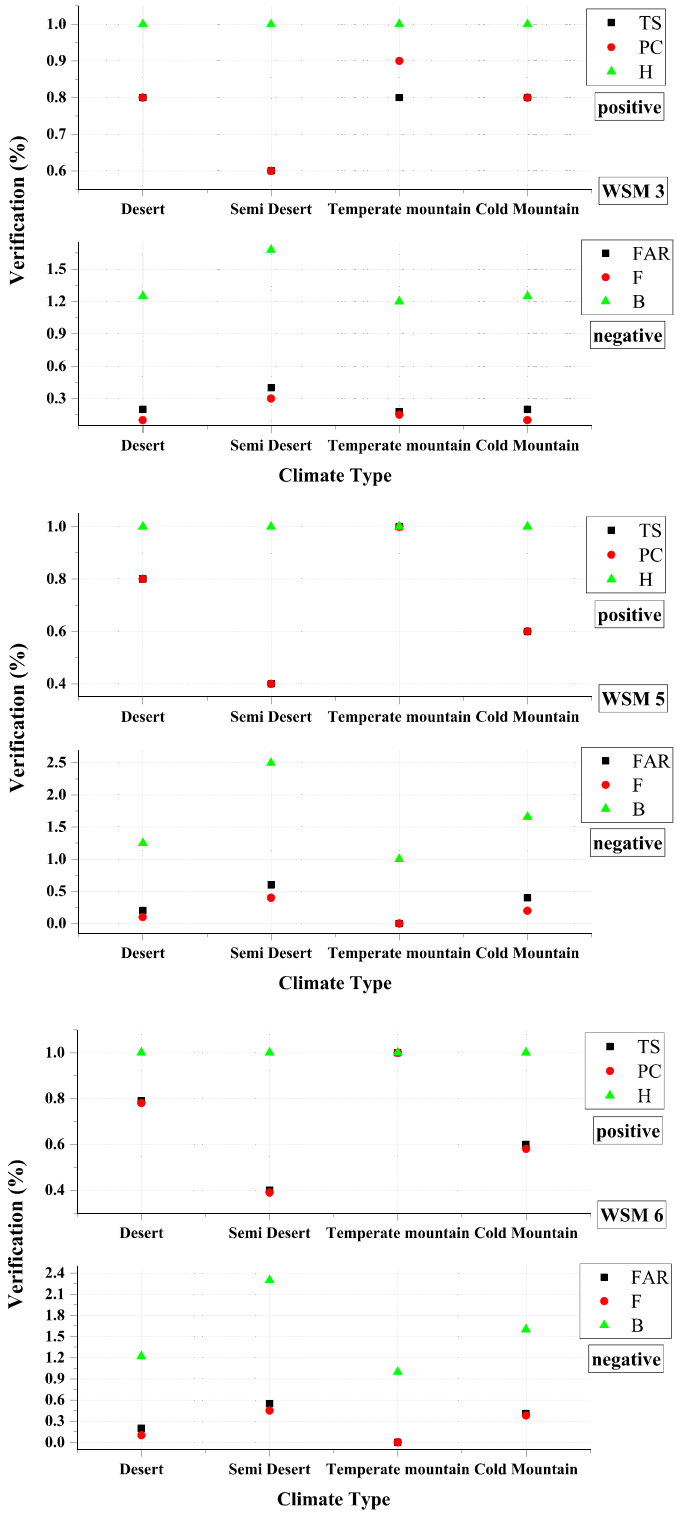

Fig. 5. (*continued*).

is ideal for simulating precipitation under the cold mountainous climatic conditions. The FAR values also show that the Lin and WDM5 schemas are the preferred, although the WDM6 and WSM3 schemas could be acceptable. Furthermore, the WDM6 and WSM3 schemas could be suitable for simulating precipitation among the positive coefficients related to the PC and TS values, although the Lin and WDM5 schemas are optimal. It is worth noting that all of the schemas are desirable depending on the coefficient H.

Table 6
The status of the evaluated schemas based on the verification results in each of the climatic types.

Climate type	Scheme	The 24-h verification results					
		Positive			Negative		
		PC	TS	H	B	FAR	F
Desert	**Lin**	*	*	*	*	*	*
	WSM6			*			
	WDM5	*	*	*	*	*	*
Semi-desert	**Lin**	*	*				
	WDM6			*			
Temperate mountainous	**Lin**	*	*	*	*	*	*
	WSM5	*	*	*	*	*	*
	WSM6	*	*	*	*	*	*
	WDM5	*	*	*	*	*	*
	WDM6	*	*	*	*	*	*
Cold mountainous	**Lin**	*	*	*	*	*	*
	WSM5	*	*	*		*	*
	WDM6	*	*	*			

*: Accepted schemas based on the amount of validation performed.

In this table, the symbol * shows the best scheme for forecasting 24-h rainfall in each of the climate representatives. The Lin schema, except for the semi-desert climate, has the best adaptability and performance in all of the climate types, according to the results of this table. As can be seen, this scheme is the most appropriate in the WRF model for simulating rainfall in most parts of the province. Except for the cold mountainous and semi-desert climate conditions, the WDM5 schema simulates rainfall accurately in most parts of the province.

Flood forecasting is one of the most severe hydrological challenges and one of the few viable flood management options. In addition, it reduces human and financial losses in many parts of the world. Finding a reliable solution to the flood forecasting problem, on the other hand, has long been regarded as one of the most serious concerns in hydrology. As a result, forecasting, planning, and management of floods require accurate rainfall estimates. Several researchers have attempted to attain this goal by employing various methods to predict rainfall accurately (Shirali et al., 2020a, 2020b).

It is necessary to employ a reliable and comprehensive method for rainfall forecasting, which necessitates implementing of early warning systems for effective flood management (Billa et al., 2004). Before the main forecast of rainfall in the study area, the five most severe flood events that have caused significant human and financial damage to the area in a given period were chosen for this study. According to the results of this study, the WRF meteorological model schemas produce varied results in various climatic conditions. For example, the WSM3, WSM5, WDM6, and WSM6 methods are unsuitable for desert climates, and all simulations considerably overestimate surface rainfall. This is consistent with Van Weverberg et al. (2013). The schemas are used without incorporating the process of ice accumulation and warm rain, which is why they simulate rainfall in desert and semi-desert areas at a lower rate than observed. Due to the presence of climate quantities compatible with desert and semi-desert climates, the Lin scheme can predict rainfall better than other schemes. In this scheme, the mixing process of precipitation particles in the atmosphere works better than other schemes for the desired climate.

Additionally, the results indicated that the best model schemas for temperate mountainous climatic conditions include those that produce the most accurate rainfall simulations when compared to other climates.

This results corroborates the findings of Qiao et al. (2018). This acceptable accuracy of the Linn scheme over temperate mountainous regions is due to the correlation and accumulation of steam, clouds, rain, ice, snow and snowflakes. There are more quantities in Lin's scheme than other schemes, which can better simulate rainfall in temperate mountainous regions. These schemas bring the results closer to reality than they would be without snow, due to the density of clouds and rain, as well as the entry of snow into the atmosphere (Hadilooie et al., 2014). According to the findings, the WRF meteorological model has an appropriate capacity for simulating rainfall in the climate types of the study area.

The values of rainfall that are simulated by the model vary depending on the scheme that is used, and some schemes produce higher values than the actual rainfall (overestimation) while some produce lower values than the actual rainfall (underestimation). However, the WRF model has the ability to simulate the rainfall in certain schemas with a minimal degree of variation from the actual value. The strength of this study is that the most earlier research (Bhimala and Gouda, 2021) has concentrated on precipitation simulation and forecasting without evaluating how precipitation quantities are employed in different climatic conditions and several regions, while the present study considers and implements it. Furthermore, the output of this meteorological model analysis can be employed in hydrological modeling that caused to rainfall-runoff forecasting in each climatic condition for the following 24 h. Another advantage of using this method is that it can assist in identifying and forecasting the occurrence of floods in different regions that have diverse climatic conditions, and it can do so in advance before the floods actually happen.

The WRF model produces the desirable accuracy results when simulating precipitation in the climate types of the study area, both temporally (24 h) and spatially (5 km resolution). The analysis of the figures demonstrates that distinct schemas should be used for each of the climatic conditions in the Khorasan Razavi Province. For example, the cities of Kashmar, Golmakan, Torbat_Jam, and Sarakhs have acceptable simulated rainfall values when compared to observational data in the semi-desert condition, whereas

Mashhad, Neyshabour, and Fariman have acceptable simulated rainfall values when compared to observational data in the temperate mountainous climatic condition (Fig. 6). This Figure shows the difference between the observational and the simulated 24-h rainfall in the events 03/24/2020 and 04/12/2020 (the most severe rainfalls). The closer the scheme values to zero, the better the scheme can used to forecast rainfall.

The relevance of employing the WRF meteorological model for rainfall simulation and forecasting is established, and the schemas are appropriately selected. For example, when the WDM5 scheme is used in Quchan, a city located in a cold mountainous climate region, the difference between simulated and observational rainfall is nearly zero, but the difference is 15 mm and 16 mm when the WSM3 and WSM6 schemas are used. Thus, the selection of scheme has an impact on the accuracy of the simulated or forecasted results. Overall, according to Fig. 6, the output of rainfall simulation show that the Lin can be used as the most desirable scheme in the study area for the forecasting process.

The results of the WRF model show that it is a robust model for simulating and forecasting rainfall, which could be particularly useful in flood forecast warnings across the various climatic regions of the study area. The inclusion of several climates in this study enhanced the results of the WRF model. This is in line with the Qiao et al. (2018) and Asghar et al. (2019).

However, its accuracy varies according to the (i) climatic conditions, (ii) the chosen scheme, and (iii) the reliability of the synoptic stations in the study area. For example, the model accurately simulates rainfall in some climate types, such as temperate mountainous and desert climates.

4. Conclusion

Flood is one of the most effective natural hazards that affect millions of people and cause huge socio-economic impacts on their life. Rainfall is the main driver of hydrological processes and flood events, and it can also trigger landslides in some areas. To reduce the human and financial impacts of floods, it is essential to simulate and forecast rainfall accurately and reliably, as this can help mitigate flood risks. Therefore, developing an accurate and reliable meteorological model is needed to estimate the spatial and temporal distribution of rainfall for hydrological applications. Accordingly, the numerical dynamic downscaling model of WRF is applied as a useful tool for rainfall simulation to determine the most desirable scheme in each of climatic type and forecast the future rainfall. The forecasted rainfall can be used for hydrological models to manage the relevant floods and mitigate the related risks, accordingly.

The purpose of this research is developing the dynamic downscaling WRF model and selecting the most desirable numerical scheme for each climatic type in the Khorasan Razavi Province, which can be used for the rainfall forecasting process for the short-time future, reliably. To achieve this goal, the six WRF model schemas including Lin, WDM5, WDM6, WSM3, WSM5, and WSM6 are compared with the observational rainfall data related to the synoptic stations of each climatic class. Consequently, according to the most acceptability based on the six verification criteria of PC, TS, H, B, FAR, and F, the most desirable scheme for each climatic type is selected. Hence, the appropriate scheme for the four different types of climates is determined.

Accordingly, the most effective five events that caused human losses and financial damages to the study area have been chosen to run the WRF model from October 2019 to May 2020. Among the selected events, the three of the events occurred on the 10/31/2019, the 03/24/2020, and the 04/12/2020 indicate the highest rainfall values. Then, the model has been verified based on the verification criteria, using the statistical calculations. Accordingly, based on the six verification results, in the desert, temperate mountainous and cold mountainous climatic conditions, the Lin scheme shows to be more compatible status in comparison with the other schemas. Also, based on the TS verification result (as the most important verification criteria), in the semi-desert climatic type, the Lin scheme has obtained the more acceptable status in comparison with the other schemas. With respect to the final results, the ability and accuracy of the WRF model for flood simulation in the study area and its local regions (the related cities) can be satisfied. Due to the fact that the study area of Khorasan Razavi province has such a diverse range of climatic conditions, the selected WRF schemas are suggested for each of these climatic conditions for the rainfall forecasting in the future. Furthermore, based on classifying the climatic regions, as well as setting the WRF model scheme for each climatic type and combining it with the hydrological and stormwater management models, the flood forecasting with adequate accuracy for the next 24 h even 72 h could be implemented.

In accordance with the limitations of the used WRF model in this study, is the overestimating of the simulated rainfall outputs in comparison with the observational data in most of the time, while just sometimes the outputs are underestimate than the observational rainfall. Also, using the dynamic downscaling model, requires to classify the climatic conditions in the local scale and select the desirable model scheme for each local region for weather simulation and its forecasting. Furthermore, due to the variety of the meteorological parameters, it should be checked several types of verification criteria including the positive and negative criteria, in the verification process. Moreover, analyzing this numerical model and getting the outputs needs using high performance computer processing, economically.

Regarding with the future studies, due to the rainfall simulation and its forecasting in the regions of the world will be combined with probable uncertainties in meteorological and hydrological modeling process, it is needed to develop comprehensive and reliable simulation/forecast numerical schemas at the regional scale depending the climatic conditions. Accordingly, it is suggested after the climatic classification at the local scale, the best meteorological model scheme is selected, then the numerical outputs of the meteorological model is used in hydrological models. According to the connection between the meteorological and hydrological models, the rainfall could be forecasted for the next 24 h, even the next 72 h and a week later, as well as the related runoff could be estimated before the critical human looses and the economical damages are occurred. Furthermore, it is suggested to combine the using of the land-based observational data and the remote sensing-based data in this dynamic downscaling numerical model for the forecasting process. Moreover, validating the statistical meteorological models with this accurate dynamic model, also validating the artificial intelligent-based forecasting methods with this numerical model is suggested.

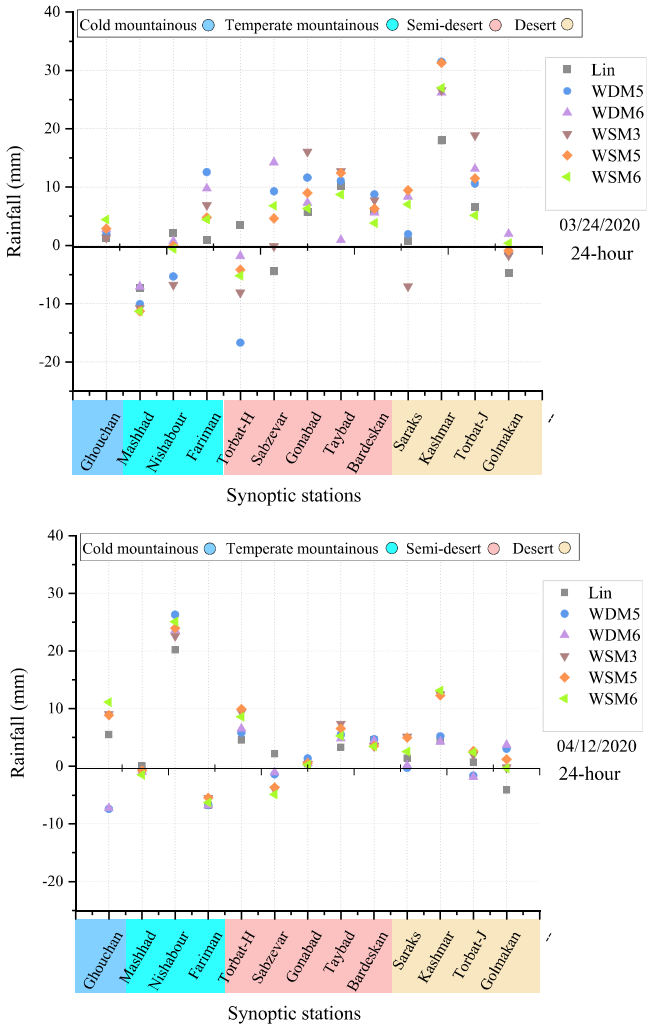

Fig. 6. The difference between the schemas output and the observational data in the climatic types for the events 03/24/2020 and 04/12/2020.

Ethics approval

Not Applicable.

Funding Statement

The authors did not receive support from any organization for the submitted work.

Availability of data and material

Not Applicable.

Code availability

Not Applicable.

Consent to participate

Not Applicable.

Consent for publication

All Authors consent to the article's publication after acceptance.

CRediT authorship contribution statement

All authors contributed to the study's conception and design. Material preparation, data collection, and analysis were performed by Rasoul Sarvestan, Mokhtar Karami and Reza Javidi Sabbaghian. The first draft of the manuscript was written by Rasoul Sarvestan and all authors carried out editing and writing and commented on previous versions of the manuscript. All authors read and approved the final manuscript.

Declaration of Competing Interest

The authors declare that they have no known competing financial interests or personal relationships that could have appeared to influence the work reported in this paper.

Data Availability

Data will be made available on request.

Appendix A. Supporting information

Supplementary data associated with this article can be found in the online version at doi:10.1016/j.ejrh.2023.101524.

References

⟨https://fa.wikipedia.org/wiki/⟩, 2019.
, 2014⟨www.mmm.ucar.edu/weather-research-and-forecasting-model⟩.
Agogbuo, C.N., Nwagbara, M.O., Bekele, E., Olusegun, A., 2017. Evaluation of selected numerical weather prediction models for a case of widespread rainfall over Central and Southern Nigeria. J. Environ. Anal. Toxicol. 7 (4), 1–9.
Alfieri, Lorenzo, Burek, Peter, Dutra, Emanuel, Krzeminski, Blazej, Muraro, David, Thielen, Jutta, Pappenberger, Florian, 2013. GloFAS-global ensemble streamflow forecasting and flood early warning. Hydrol. Earth Syst. Sci. 17, 1161.
Andimuthu, Ramachandran, Kandasamy, Palanivelu, Mudgal, B.V., Jeganathan, Anushiya, Balu, Abinaya, Sankar, Guganesh, 2019. Performance of urban storm drainage network under changing climate scenarios: flood mitigation in Indian coastal city. Sci. Rep. 9 (1), 10.
Asghar, Malik Rizwan, Ushiyama, Tomoki, Riaz, Muhammad, Miyamoto, Mamoru, 2019. Flood and inundation forecasting in the sparsely gauged transboundary Chenab river basin using satellite rain and coupling meteorological and hydrological models. J. Hydrometeorol. 20, 2315–2330.
Bhimala, Kantha Rao, Gouda, Krushna Chandra, 2021. Evaluating the spatial distribution of WRF-simulated rainfall, 2-m air temperature, and 2-m relative humidity over the urban region of Bangalore, India. Pure Appl. Geophys. 178, 1105–1120.
Billa, Lawal, Mansor, Shattri, Rodzi Mahmud, Ahmad, 2004. Spatial information technology in flood early warning systems: an overview of theory, application and latest developments in Malaysia. Disaster Prev. Manag.: Int. J.
Cao, Qimin, Jiang, Baolin, Shen, Xiaodian, Lin, Wenshi, Chen, Junwen, 2021. Microphysics effects of anthropogenic aerosols on urban heavy precipitation over the Pearl River Delta, China. Atmos. Res. 253, 105478.
Casagli, N., Dapporto, S., Ibsen, M.L., Tofani, V., Vannocci, P., 2006. Analysis of the landslide triggering mechanism during the storm of 20th–21st November 2000, in Northern Tuscany. Landslides 3, 13–21.
Chen, Xiaodong, Hossain, Faisal, 2018. Understanding model-based probable maximum precipitation estimation as a function of location and season from atmospheric reanalysis. J. Hydrometeorol. 19, 459–475.
Clark, C., Dent, J., 2021. New estimates of 24-h probable maximum precipitation (PMP) for the British Isles. J. Geosci. Environ. Prot. 9 (7), 209–228.
Cluckie, I.D., Han, D., 2000. Fluvial flood forecasting. Water Environ. J. 14, 270–276.
Cong, Xiang-yu, Ni, Guang-heng, Hui, Shi-bo, Tian, Fu-Qiang, Zhang, Tong, 2006. Simulative analysis on storm flood in typical urban region of Beijing based on SWMM. Water Resour. Hydropower Eng. 4, 64–67.
Dhib, Saoussen, Homar, Víctor, Bargaoui, Zoubeida, Vich, Mariadelmar, 2021. Sensitivity of the Weather Research and Forecasting model (WRF) to downscaling extreme events over Northern Tunisia. Nat. Hazards Earth Syst. Sci. Discuss. 1–27.
Douinot, Audrey, Roux, Hélène, Garambois, Pierre-André, Larnier, Kévin, Labat, David, Dartus, Denis, 2016. Accounting for rainfall systematic spatial variability in flash flood forecasting. J. Hydrol. 541, 359–370.
El Afandi, Gamal, Morsy, Mostafa, 2020. Developing an early warning system for flash flood in Egypt: case study the Sinai Peninsula. in: Flash Floods in Egypt (Springer).
Evans, James E., Mackey, Scudder D., Gottgens, Johan F., Gill, Wilfrid M., 2000. Lessons from a dam failure.
Faiers, G., Keim, B.D., Hirschboeck, K.K., 1994. A synoptic evaluation of frequencies and intensities of extreme three-and 24-h rainfall in Louisiana. Prof. Geogr. 46 (2), 156–163.
Fatti, Elizabeth, Christina, Patel, Zarina, 2013. Perceptions and responses to urban flood risk: implications for climate governance in the South. Appl. Geogr. 36, 13–22.
Gbode, I.E., Dudhia, J., Ogunjobi, K.O., Ajayi, V.O., 2019. Sensitivity of different physics schemes in the WRF model during a West African monsoon regime. Theor. Appl. Climatol. 136 (1), 733–751.
Givati, Amir, Lynn, Barry, Liu, Yubao, Rimmer, Alon, 2011. Using the WRF model in an operational streamflow forecast system for the Jordan River. J. Appl. Meteorol. Climatol. 51, 285–299.
Guo, Jiaxu, Lei, Hengchi, Chen, Di, Yang, Jiefan, 2019. Evaluation of the WDM6 scheme in the simulation of number concentrations and drop size distributions of warm-rain hydrometeors: comparisons with the observations and other schemes. Atmos. Ocean. Sci. Lett. 12, 458–466.

Hadilooie, Hassan, Azadi, Majid, Memarian, Mohammad, Mohammad, M., 2014. Evaluating the Performance of WRF Cloud Microphysical Schemes (Thesis Submitted for the Degree of M. Sc. in Meteorology), pp. 1–92.
Hong, S.-Y., Dudhia, J., Chen, S.-H., 2004. A revised approach to ice microphysical processes for the bulk parameterization of clouds and precipitation. Monthly weather review 132 (1), 103–120.
Hong, Song-You, Lim, Jeong-Ock Jade, 2006. The WRF single-moment 6-class microphysics scheme (WSM6). Asia-Pac. J. Atmos. Sci. 42, 129–151.
Hong, Song-You, Lim, Kyo-Sun Sunny, Lee, Yong-Hee, Ha, Jong-Chul, Kim, Hyung-Woo, Ham, Sook-Jeong, Dudhia, Jimy, 2010. Evaluation of the WRF double-moment 6-class microphysics scheme for precipitating convection. Adv. Meteorol. 2010.
Jain, Sharad Kumar, Mani, Pankaj, Jain, Sanjay K., Prakash, Pavithra, Singh, Vijay P., Tullos, Desiree, Kumar, Sanjay, Agarwal, S.P., Dimri, A.P., 2018. A Brief review of flood forecasting techniques and their applications. Int. J. River Basin Manag. 16, 329–344.
Jha, Manoj K., Afreen, Sayma, 2020. Flooding urban landscapes: analysis using combined hydrodynamic and hydrologic modelling approaches. Water 12, 1986.
Karki, R., ul Hasson, S., Gerlitz, L., Talchabhadel, R., Schenk, E., Schickhoff, U., Scholten, T., Böhner, J., 2018. WRF-based simulation of an extreme precipitation event over the Central Himalayas: atmospheric mechanisms and their representation by microphysics parameterization schemes. Atmos. Res. 214, 21–35.
Khalili, A., Hajam, I., Parviz, I., 1991. Comprehensive Water Plan of the Country, Climate Divisions. Ministry of Energy Publications.
Khan, Sadiq I., Hong, Yang, Gourley, Jonathan J., Khattak, Muhammad Umar, De Groeve, Tom, 2014. Multi-sensor imaging and space-ground cross-validation for 2010 flood along Indus River, Pakistan. Remote Sens. 6, 2393–2407.
Khansalari, S., Ranjbar-Saadatabadi, A., Fazel-Rastgar, F., Raziei, T., 2021. Synoptic and dynamic analysis of a flash flood-inducing heavy rainfall event in arid and semi-arid central-northern Iran and its simulation using the WRF model. Dyn. Atmos. Oceans 93, 101198.
Kodamana, Rithwik, Fletcher, Christopher G., 2021. Validation of CloudSat-CPR derived precipitation occurrence and phase estimates across Canada. Atmosphere 12, 295.
Langkamp, T., Böhner, Jürgen, 2011. Influence of the compiler on multi-CPU performance of WRFv3. Geosci. Model Dev. 4, 611–623.
Letson, F., Shepherd, T., Barthelmie, R., Pryor, S., 2020. Modelling hail and convective storms with WRF for wind energy applications. J. Phys.: Conf. Ser. (Paper presented at the).
Liu, J., Bray, M., Han, D., 2013. A study on WRF radar data assimilation for hydrological rainfall prediction. Hydrol. Earth Syst. Sci. 17, 3095.
Liu, Jia, Bray, Michaela, Han, Dawei, 2012. Sensitivity of the Weather Research and Forecasting (WRF) model to downscaling ratios and storm types in rainfall simulation. Hydrol. Process. 26, 3012–3031.
Mahala, B., Mohanty, P., Nayak, B., Mahala, B., 2015. Impact of microphysics schemes in the simulation of cyclone phailinusing WRF model. Procedia Eng. 116, 655–662.
Mahala, Biranchi Kumar, Mohanty, Pratap Kumar, Xalxo, Kanak Lata, Routray, Ashish, Misra, Satya Kumar, 2021. Impact of WRF parameterization schemes on track and intensity of extremely severe cyclonic storm "Fani". Pure Appl. Geophys. 178, 245–268.
Masaki, Yoshimitsu, Hanasaki, Naota, Takahashi, Kiyoshi, Hijioka, Yasuaki, 2014. Global-scale analysis on future changes in flow regimes using Gini and Lorenz asymmetry coefficients. Water Resour. Res. 50, 4054–4078.
Mekawy, M., Saber, M., Mekhaimar, S.A., Zakey, A.S., Robaa, S.M., Abdel Wahab, M., 2022. Evaluation of WRF microphysics schemes performance forced by reanalysis and satellite-based precipitation datasets for early warning system of extreme storms in hyper arid environment. Climate 11 (1), 8.
Meteorological, 2020. Meteorological Organization of Iran.
Mishra, V., Dominguez, F., Lettenmaier, D.P., 2012. Urban precipitation extremes: how reliable are regional climate models? Geophys. Res. Lett. 39 (3).
Mohammadiha, Amir, Memarian, Mohammad, Azadi, Majid, Parvari, Reyhani, 2012. Verification of WRF Model Forecasting for the Content of Precipitable Water and Precipitation with the RADAR Data (Thesis submitted For the degree of M.Sc), pp. 1–160.
Naing, Su Myat, 2021. Sensitivity Analysis of Heavy Rainfall Events on Physical Parameterization Configurations Using WRF-ARW Model over Myanmar.
Osman, M., Zittis, G., Haggag, M., Abdeldayem, A.W., Lelieveld, J., 2021. Optimizing regional climate model output for hydro-climate applications in the Eastern Nile Basin. Earth Syst. Environ. 5 (2), 185–200.
Pellicone, Gaetano, Caloiero, Tommaso, Guagliardi, Ilaria, 2019. The De Martonne aridity index in Calabria (Southern Italy). J. Maps 15, 788–796.
Peterson, Eric W., Wicks, Carol M., 2006. Assessing the importance of conduit geometry and physical parameters in karst systems using the stormwater management model (SWMM). J. Hydrol. 329, 294–305.
Qiao, Xiaoshi, Wang, Shizhang, Min, Jinzhong, 2018. The impact of a stochastically perturbing microphysics scheme on an idealized supercell storm. Mon. Weather Rev. 146, 95–118.
Sarvestan, R., Karami, M., Javidi Sabbaghian, R., 2023. Spatial analysis and optimization of raingauge stations network in urban catchment using weather research and forecasting model. Theor. Appl. Climatol. 153, 573–591.
Satya, O.C., Kaban, H., Irfan, M., Rahmasari, K., Monica, C., Sari, D. Mandahiling, P. 2021. Evaluation of several cumulus parameterization schemes for daily rainfall predictions over Palembang City. Paper presented at the Journal of Physics: Conference Series.
Shirali, Emadeddin, Fathian, Hosein, Zohrabi, Narges, Hassan, Elham Mobarak, 2020b. Evaluation of WRF model for simulation of precipitation and flood forecasting in Karun 4 basin. Iran. J. Soil Water Res. 51, 1907–1920.
Shirali, Emadeddin, Shahbazi, Alireza Nikbakht, Fathian, Hossein, Zohrabi, Narges, Hassan, Elham Mobarak, 2020a. Evaluation of WRF and artificial intelligence models in short-term rainfall, temperature and flood forecast (case study). J. Earth Syst. Sci. 129, 1–16.
Skamarock, W.C., Klemp, J.B., Dudhia, J., Gill, D.O., Barker, D.M., Duda, M.G., Huang, X.Y.W., Wang Powers, J.G., 2008. A description of the advanced research WRF Version 3, 125pp', NCAR Tech. Note NCAR/TN-475+ STR.
Skamarock, William C., Klemp, J.B., Dudhia, J., Gill, D.O., Barker, D.M., Wang, W., Powers, J.G., 2005. A description of the Advanced Research WRF version 2. NCAR Tech. In.: Note NCAR/TN-4681STR.
Sofokleous, I., Bruggeman, A., Michaelides, S., Hadjinicolaou, P., Zittis, G., Camera, C., 2021. Comprehensive methodology for the evaluation of high-resolution WRF multiphysics precipitation simulations for small, topographically complex domains. J. Hydrometeorol. 22 (5), 1169–1186.
Statistical yearbook, Khorasan Razavi province, 2019. Land and Climate. Statistics Center of Iran, pp. 115–25.
Tabari, Hossein, Hosseinzadeh Talaee, P., Mousavi Nadoushani, S.S., Willems, Patrick, Marchetto, Aldo, 2014. A survey of temperature and precipitation based aridity indices in Iran. Quat. Int. 345, 158–166.
Thakur, Praveen K., Roy, Adrija, Aggarwal, S.P., Nikam, Bhaskar R., Garg, Vaibhav, Kumar, A. Senthil, Chouksey, Arpit, Dhote, Pankaj, Jha, Ashutosh, 2018. Flood early warning and vulnerability assessment using Integration of weather forecasting, hydrological and geospatial modeling in North-Western Himalaya river basins. 42nd COSPAR Scientific Assembly. vol. 42, A3. 1–46-18.
Tian, Jiyang, Liu, Jia, Yan, Denghua, Ding, Liuqian, Li, Chuanzhe, 2019. Ensemble flood forecasting based on a coupled atmospheric-hydrological modelling system with data assimilation. Atmos. Res. 224, 127–137.
Van Weverberg, Kwinten, Vogelmann, A.M., Lin, W., Luke, E.P., Cialella, A., Minnis, P., Khaiyer, M., Boer, E.R., Jensen, M.P., 2013. The role of cloud microphysics parameterization in the simulation of mesoscale convective system clouds and precipitation in the tropical western Pacific. J. Atmos. Sci. 70, 1104–1128.
Wang, Jun, Huang, Bormin, Huang, Allen, Goldberg, Mitchell D., 2011. Parallel computation of the Weather Research and Forecast (WRF) wdm5 cloud microphysics on a many-core GPU. In: Proceedings of the 2011 IEEE 17th International Conference on Parallel and Distributed Systems. IEEE, pp. 1032–37.
Wong, D.C., Pleim, J., Mathur, R., Binkowski, F., Otte, T., Gilliam, R., Pouliot, G., Xiu, A., Young, J.O., Kang, D., 2012. WRF-CMAQ two-way coupled system with aerosol feedback: software development and preliminary results. Geosci. Model Dev. 5, 299–312.
Wu, Juan, Lu, Guihua, Wu, Zhiyong, 2014. Flood forecasts based on multi-model ensemble precipitation forecasting using a coupled atmospheric-hydrological modelling system. Nat. Hazards 74, 325–340.
Xiefei, Z., Chen, Z., 2020. Heavy precipitation forecasts based on multi-model ensemble members, vol. 31(no. 3), pp. 303–14.
Yesubabu, Viswanadhapalli, Srinivas, Challa Venkata, Langodan, Sabique, Hoteit, Ibrahim, 2016. Predicting extreme rainfall events over Jeddah, Saudi Arabia: impact of data assimilation with conventional and satellite observations. Q. J. R. Meteorol. Soc. 142, 327–348.

Zahmatkesh, Z, Karamouz, M, Goharian, E, Burian, S.J., 2015. Analysis of the effects of climate change on urban stormwater runoff using statistically downscaled precipitation data and a change factor approach. J. Hydrol. Eng. 20, 05014022.
Zanjani, M., Sufi, M., 2016. Investigating the shape-climatology characteristics of ditches in order to classify ditched areas in Zanjan province. Watershed research 26 (2), 1–10.
Zeyaeyan, S., Fattahi, E., Ranjbar, A., Azadi, M., Vazifedoust, M., 2017. Evaluating the effect of physics schemes in WRF simulations of summer rainfall in northwest Iran. Climate 5, 48.
Zhang, Lei, Gong, Sunling, Zhao, Tianliang, Zhou, Chunhong, Wang, Yuesi, Li, Jiawei, Ji, Dongsheng, He, Jianjun, Liu, Hongli, Gui, Ke, 2021. Development of WRF/CUACE v1. 0 model and its preliminary application in simulating air quality in China. Geosci. Model Dev. 14, 703–718.